

Article

Preparation and Single Crystal Structure Determination of the First Biobased Furan-Polydiacetylene Using Topochemical Polymerization

Yves L. Dory ¹, Mia Caron ², Vincent Olivier Duguay ², Lucas Chicoine-Ouellet ², Daniel Fortin ³ and Pierre Baillargeon ^{2,*}

¹ Laboratoire de Synthèse Supramoléculaire, Département de Chimie, Institut de Pharmacologie, Université de Sherbrooke, 3001 12e Avenue Nord, Sherbrooke, QC J1H 5N4, Canada

² Département de Chimie, Cégep de Sherbrooke, 475 Rue du Cégep, Sherbrooke, QC J1E 4K1, Canada

³ Laboratoire d'Analyses Structurales par Diffraction des Rayons-X, Département de Chimie, Université de Sherbrooke, 2500, Boulevard de l'Université, Sherbrooke, QC J1K 2R1, Canada

* Correspondence: Pierre.Baillargeon@cegepsherbrooke.qc.ca; Tel.: +1-819-564-6350-4114

Received: 31 July 2019; Accepted: 28 August 2019; Published: 29 August 2019



Abstract: Crystal structure elucidations of bio-based polymers provide invaluable data regarding structure–property relationships. In this work, we achieved synthesis and Single Crystal X-ray Diffraction (SCXRD) structural determination of a new furan-based polydiacetylene (PDA) derivative with carbamate (urethane) functionality. Firstly, diacetylene (DA) monomers were found to self-assemble in the crystalline state in such a way that the polymerization theoretically occurred in two different directions. Indeed, for both directions, geometrical parameters for the reactive alignment of DA are satisfied and closely related with the optimal geometrical parameters for DA topochemical polymerization ($d(1) = 4.7\text{--}5.2 \text{ \AA}$, $d(2) \leq 3.8 \text{ \AA}$, $\theta \approx 45^\circ$). However, within the axis of hydrogen bonds (HB), the self-assembling monomers display distances and angles ($d(1) = 4.816 \text{ \AA}$, $d(2) = 3.822 \text{ \AA}$, $\theta = 51^\circ$) that deviate more from the ideal values than those in the perpendicular direction ($d(1) = 4.915 \text{ \AA}$, $d(2) = 3.499 \text{ \AA}$, $\theta \approx 45^\circ$). As expected from these observations, the thermal topochemical polymerization occurs in the direction perpendicular to the HB and the resulting PDA was characterized by SCXRD.

Keywords: biopolymer; sustainable materials; polydiacetylene; furan; Single Crystal X-ray Diffraction (SCXRD); carbamate; hydrogen bond; topochemical polymerization; diacetylene

1. Introduction

Biomass and biomass-derived materials are considered by the scientific community as some of the most promising alternatives for decreasing the current dependence on fossil resources [1–6]. This is evidenced by plans to gradually replace some petroleum-based plastic by bio-based plastic [7–12] or at least hybrid bio- and fossil-based polymeric blends [13,14]. Synthesis of bio-based polymers, especially furan-based polymers, has, therefore, been the subject of extensive studies [15–23]. There are several reasons that can explain the growing interest in furan-based polymers: (1) they originate from lignocellulose, the most abundant and bio-renewable biomass on earth [1]; (2) the synthetic accessibility of a wide variety of furan monomers with very different chemical properties, providing access to various types of macromolecular materials such as polyesters, polyamides, polyurethanes, epoxy resins, etc., [18]; and (3) the possibility of exploiting the chemical features associated with the

furan heterocycle (e.g., thermoreversible furan/maleimide Diels-Alder reaction) to prepare materials with useful properties, such as self-healing, thermal reverse-cross-linking and recyclability [3,24,25].

Development of new bio-based polymers requires characterization tools to gain better understanding of the material's structure and properties [26]. In this context, X-ray Diffraction (XRD) techniques are widely applied [27–29]. These effective tools were also exploited in the case of furan-based polymers, which have been studied by many X-ray characterization techniques such as X-ray Powder Diffraction (XRPD) [30], X-ray Fiber Diffraction (XRFD) [31], Wide-Angle X-ray Scattering (WAXS) [32], and Small-Angle X-ray Scattering (SAXS) [33]. In this way, the herringbone packing of polyfuran, a semiconducting polymer, has been indirectly inferred from the related α -sexifuran single crystal structure (Figure 1a) [34,35]. The same Single Crystal X-ray Diffraction (SCXRD) technique was also used to predict the potential biological activities of a newly developed BisFuran Diol (BFD, Figure 1b) from a structural comparison with the famous endocrine disruptor bisphenol A (BPA) [36]. Finally, the structure of a furfural-derived diacid monomer (CBDA-2) prepared with a solid-state [2+2] photocycloaddition (Figure 1c) was also explored using SCXRD. That rigid monomer was later introduced in a fully bio-based polymer through condensation with glycerol [37].

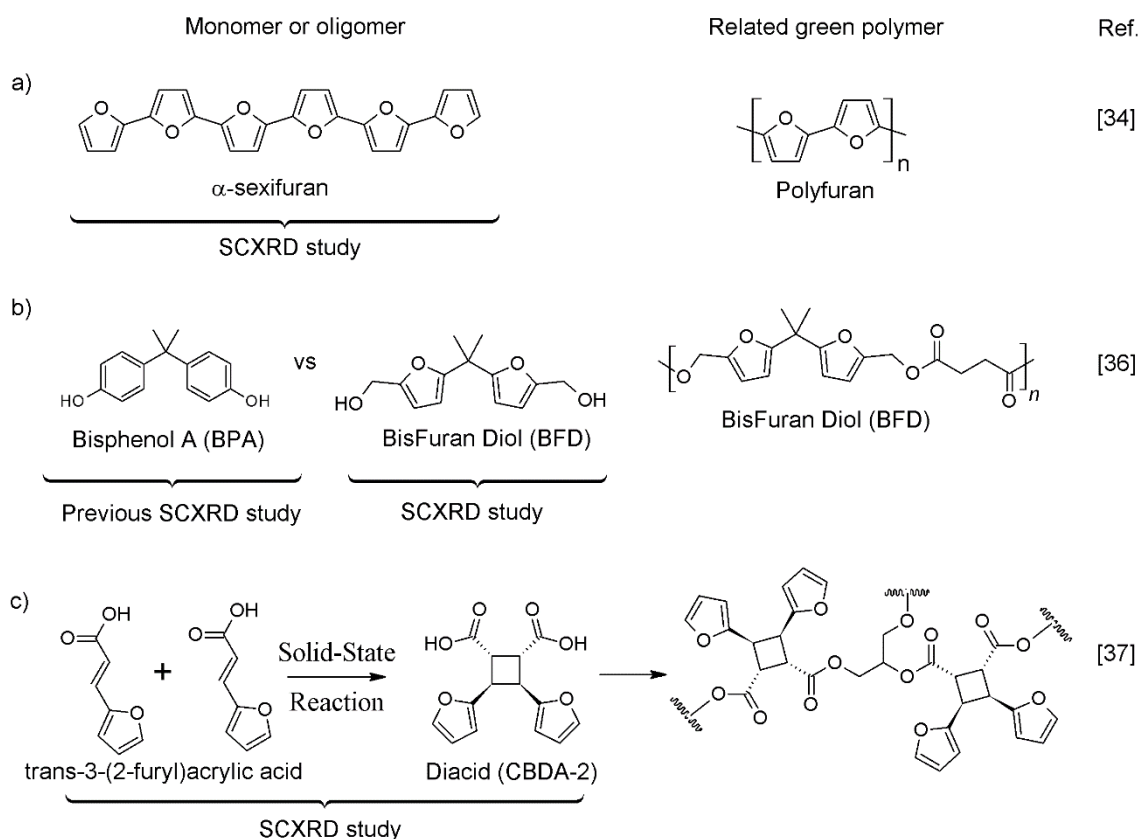


Figure 1. Some selected examples of furan-based monomer or oligomer investigated using Single Crystal X-ray Diffraction (SCXRD) technique. (a) α -sexifuran, (b) BisFuran Diol (BFD), and (c) diacid (CBDA-2)

However, to the best of our knowledge, there is no single example of a complete SCXRD characterization of a furan-based polymer. While some natural furan-based diacetylene (DA) do exist [38–40], no attempts to polymerize them have been reported. This seems quite surprising since polydiacetylene (PDA) has attracted tremendous attention for applications in various fields [41,42] due to its unique chromatic [43–50] and semi-conductive properties [51–61].

We now present the complete SCXRD structural determination of the thermal topochemical polymerization of the furan-DA derivative **1** to the semiconducting Furan-PDA **2** (Figure 2). As already

documented, the general polymerization of DA in the solid-state proceeds only if specific geometrical and experimental conditions are fulfilled [62–66]. The SCXRD analysis of this process is useful since it provides valuable data for the comprehension of the structure–property relationships within materials.

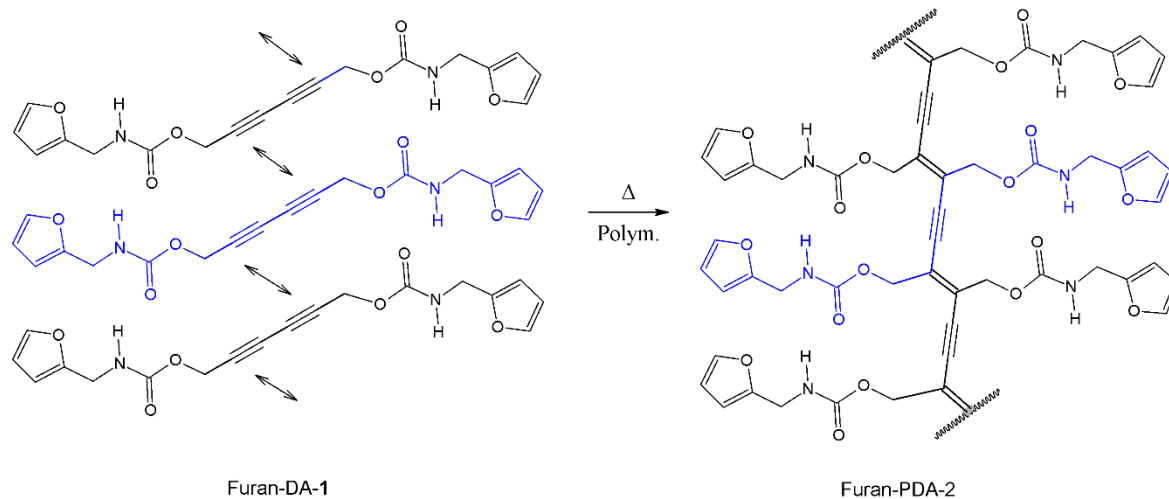
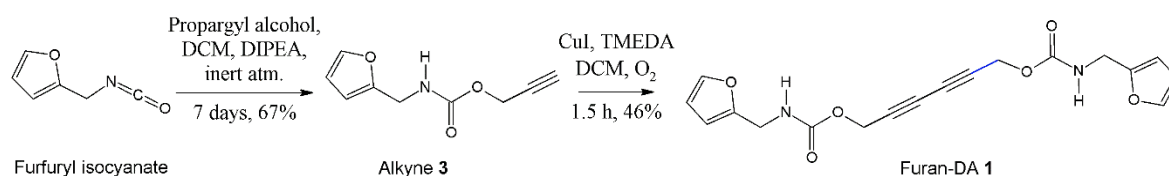


Figure 2. Chemical structures of the furan-diacetylene (DA) derivative **1** and the corresponding furan-polydiacetylene (PDA) **2** which have both been fully characterized using SCXRD.

2. Materials and Methods

2.1. Synthesis and Recrystallization

Alkyne **3** was obtained in an efficient manner from commercially available furfuryl isocyanate (Scheme 1). The homocoupling of the isolated terminal alkyne **3** to give symmetrical Furan-DA **1** was achieved in 1.5 h with a Hay catalyst [67]. All chemicals were handled with great care as the Furan-DA **1** is sensitive to light and temperature.



Scheme 1. Synthesis of alkyne **3** and symmetrical Furan-DA **1**. DCM: dichloromethane; DIPEA: diisopropylethylamine; TMEDA: tetramethylethylenediamine.

2.1.1. Synthesis of Alkyne **3**

To a solution of propargyl alcohol (130 μ L, 2.27 mmol) in dichloromethane (DCM, 10 mL) were added furfuryl isocyanate (175 μ L, 1.62 mmol) and *N,N*-diisopropylethylamine (DIPEA, 340 μ L, 1.95 mmol) under argon. The reaction mixture was stirred under an argon atmosphere for seven days at room temperature. The resulting mixture was purified by flash chromatography (DCM then 1% Acetone/DCM), yielding the alkyne **3** as an orange oil which slowly solidified (196 mg, 67%). *R*_f = 0.35 (DCM). ¹H NMR (300 MHz, CDCl₃) δ ppm: 7.30 (d, 1H, *J* = 1.8 Hz), 6.26 (m, 1H), 6.18 (d, 1H, *J* = 3.3 Hz), 5.53 (br, 1H), 4.63 (d, 2H, *J* = 2.7 Hz), 4.29 (d, 2H, *J* = 6.0 Hz), and 2.44 (t, 1H, *J* = 2.7 Hz).

2.1.2. Synthesis and Recrystallization of Furan-DA **1**

To a solution of alkyne **3** (495 mg, 2.76 mmol) in DCM (8 mL), Hay catalyst was added. The catalyst had been freshly prepared by stirring CuI (534 mg, 2.76 mmol) and tetramethylethylenediamine (TMEDA, 830 μ L, 5.53 mmol) in DCM (7 mL) under argon. The reaction vessel was then covered

with aluminum foil to prevent early photopolymerization. The reaction mixture was stirred under an oxygen atmosphere (balloon) for 90 min, before it was then passed through a short pad of silica gel, applying a gradient of solvent from pure DCM to 1% acetone/DCM, then to 5% acetone/DCM. The solvent was removed under reduced pressure while keeping the temperature below 45 °C to prevent thermal polymerization. The resulting Furan-DA **1** appeared as a white solid with a slight purple tint (≈ 225 mg, $\approx 46\%$), that was quickly dissolved in a minimal volume of DCM. A small amount of red insoluble fibers (presumably Furan-PDA **2**) was filtered off (cotton wool), before pentane was allowed to slowly diffuse in the DCM solution of **1** at 5 °C. Pink-colored single crystals of Furan-DA **1**, with plate and needle morphologies, suitable for X-ray analysis, were harvested. $R_f = 0.05$ (DCM) and 0.43 (5% acetone/DCM). $^1\text{H NMR}$ (300 MHz, CDCl_3) δ ppm: 7.35 (m, 1H), 6.31 (m, 1H), 6.23 (m, 1H), 5.12 (br, 1H), 4.76 (s, 2H), and 4.36 (d, 2H, $J = 6.0$ Hz).

2.2. Topochemical Polymerization of Furan-DA **1** to Afford Furan-PDA **2**

After one week at room temperature, the initial clear pink crystals of Furan-DA **1** had turned into deeper red–purple crystals, providing evidence of PDA formation that is visible to the naked eye. In order to drive the topochemical polymerization to completeness, the crystals were heated at 80 °C for 50 h, then subsequently, at 65 °C for 20 h. The resulting lustrous dark red needle-like single crystals of Furan-PDA **2** were suitable for X-ray analysis.

2.3. Single Crystal Structure Analysis of Furan-DA **1** and Furan-PDA **2**

The X-ray intensity data were measured on a Bruker Apex DUO system equipped with a Cu $K\alpha$ ImuS micro-focus source with MX optics ($\lambda = 1.54178$ Å). The frames were integrated with the Bruker SAINT software package using a wide-frame algorithm. Data were corrected for absorption effects using the Numerical Mu Calculated method (SADABS). The structure was solved and refined using the Bruker SHELXTL Software Package. Details of the crystallographic data and refinement are presented in Table 1 and in the Supplementary Materials (CIF). Crystallographic data for the structures reported in this paper have also been deposited in the Cambridge Crystallographic Data Centre (CCDC). The following numbers CCDC-1922071 and CCDC-1922076 have been assigned to the two compounds Furan-DA **1** and Furan-PDA **2**, respectively.

Table 1. Crystallographic data for Furan-DA **1** and Furan-PDA **2**.

	Furan-DA 1	Furan-PDA 2
formula	$\text{C}_{18}\text{H}_{16}\text{N}_2\text{O}_6$	$(\text{C}_{18}\text{H}_{16}\text{N}_2\text{O}_6)_n$
CCDC Number	1922071	1922076
MW/g mol ⁻¹	356.33	356.33
crystal color	clear light pink	lustrous dark red
crystal system	monoclinic	monoclinic
space group	$P2_1/c$	$P2_1/c$
$a/\text{Å}$	4.9153(3)	4.8908(1)
$b/\text{Å}$	38.0403(19)	37.6027(9)
$c/\text{Å}$	4.8163(2)	4.8297(1)
β/deg	109.884(4)	112.000(1)
$V/\text{Å}^3$	846.86(8)	823.54(3)
Z	2	2
density (calculated)/g cm ⁻³	1.397	1.437
total number of reflections	8755	10411
independent reflections	1548	1544
R_{int}	0.0842	0.0717
$R_1 [I > 2\sigma(I)]$	0.0863	0.0524
$wR_2 [I > 2\sigma(I)]$	0.1696	0.1295
GoF	1.100	1.077

3. Results and Discussion

3.1. Single Crystal Structure of Furan-DA 1

All the hydrogen bond (HB) capabilities arising from the carbamate $C=O$ and $N-H$ parts are fulfilled in the crystal of Furan-DA 1. As a result, each C_i symmetric unit 1 is involved in four HBs with two neighbors. In this arrangement, parallel stacking of carbamates causes the alignment of diynes parallel to the c -axis (Figure 3a). Such alignment of diynes is also present along the perpendicular a -axis despite the absence of HBs (Figure 3b). In both cases, the distance $d(2)$ between the diynes reactive carbons, which is under 4 \AA , is in fairly good agreement with the optimal value for the 1,4-addition reaction [65,68] (Table 2). However, the closer $d(2)$ contact for the a -axis values in the case of the DA stacking in the perpendicular direction to the hydrogen bonding seems to be more prone to polymerization. Another argument in favor of the polymerization in the ab plane is that the solid-state reaction needs to proceed with a certain degree of flexibility between the reactive monomers. In some cases, the additional rigidity from the presence of intermolecular hydrogen bonds has been reported to inhibit the solid-state reactivity [69]. The same phenomenon has been reported for a similar DA in which the biobased furan group of 1 had been replaced by a benzyl group [70].

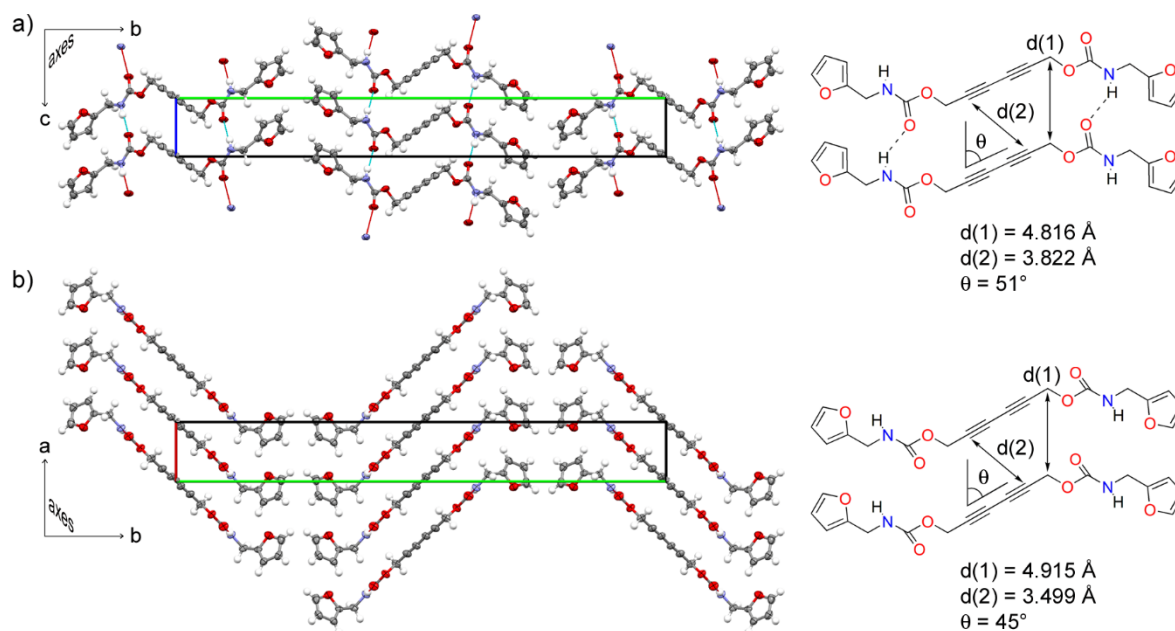


Figure 3. Alignment of diacetylene functional groups in the stacking of Furan-DA 1 (a) parallel to the c -axis and (b) parallel to the a -axis.

Table 2. Comparison between the general optimal values for topochemical polymerization and the geometrical parameter observed for the stacking of Furan-DA 1 in the direction parallel to the c -axis (parallel to the hydrogen bonds (HBs)) and parallel to the a -axis (orthogonal to the HBs).

Significant Geometric Parameters for Polymerization of DA	Optimal Values	Furan-DA 1 (Direction Parallel to the c -axis)	Furan-DA 1 (Direction Parallel to the a -axis)
$d(1)$	$4.7\text{--}5.2 \text{ \AA}$	4.816 \AA	4.915 \AA
$d(2)$	$\leq 3.8 \text{ \AA}$	3.822 \AA	3.499 \AA
θ	$\approx 45^\circ$	51°	45°

3.2. Topochemical Polymerization of Furan-DA 1 to Furan-PDA 2

As expected from the topological parameters (Table 2), the topochemical thermal polymerization of Furan-DA 1 proceeds within the ab plane (Figure 4). The product Furan-PDA 2 is, as often observed for symmetric DAs, the result of a turnstile mechanism [63], which leads to contraction (about 1.2%)

along the *b*-axis (38.0403 to 37.6027 Å). Looking in the *a*-axis direction, the repeating period *d*(1) also shrinks from 4.9153 to 4.8908 Å (about 0.5% only). In this context, the furan side groups stay at almost the same position before and after the solid-state transformation, ensuring a smooth transition.

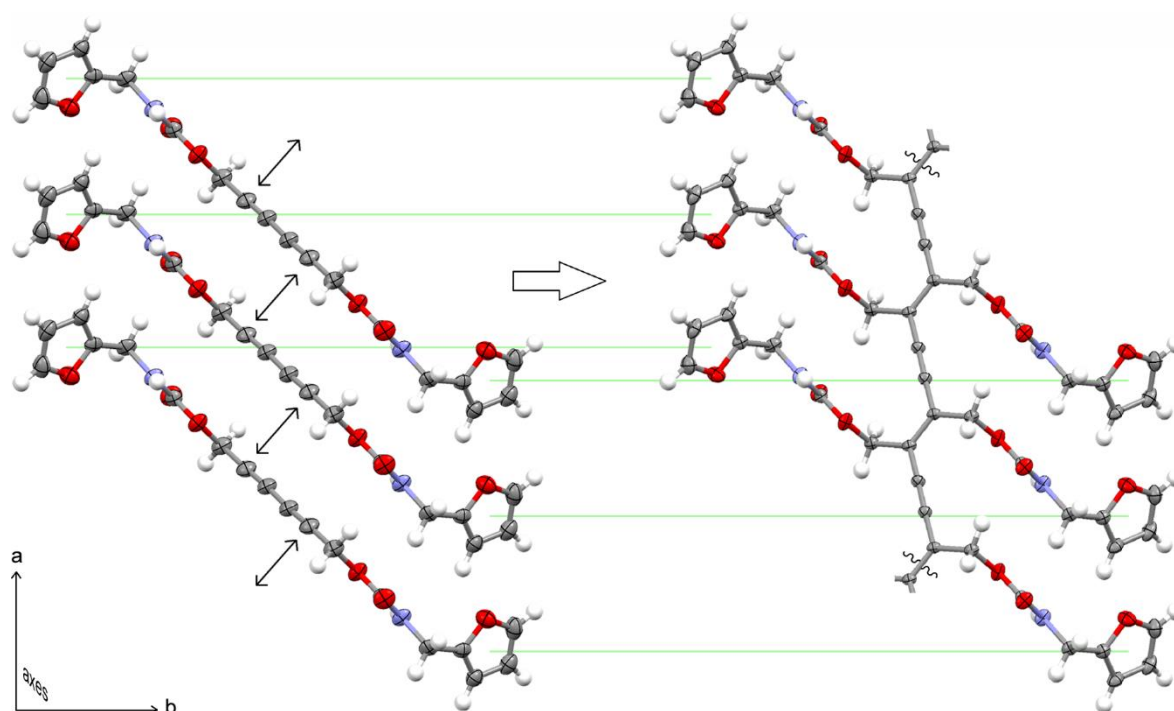


Figure 4. Single crystal characterization of the topochemical polymerization of Furan-DA **1** to Furan-PDA **2**.

A small expansion from 4.8163 to 4.8297 Å (about 0.3%) was observed along the *c*-axis (the direction of the HBs). There is also a minor change in the hydrogen bond distance contact ($\text{N-H} \dots \text{O}$), which corresponds to 2.859 Å in the monomer crystal and 2.863 Å in the final PDA crystal. As the H-bonding pattern is nearly unaffected, almost no lattice strain or mismatch is present and the polymerization can proceed smoothly to completion [70]. Finally, although the *c*-axis shows an expansion, the resulting final PDA crystal is denser than the corresponding DA monomer crystal (respectively, 1.437 vs. 1.397 g/cm³, Table 1).

4. Conclusions

Furan-based biopolymers have received considerable attention in recent years because of their great potential to replace petroleum-based plastics [11]. Organic Semiconductor Single Crystals [58,71,72] are also considered to be an important research topic, given they are “ideal candidates for the construction of high-performance optoelectronic devices/circuits” [55]. In this study, we reported the topochemical polymerization of a furan-based diacetylene (Furan-DA **1**). In fact, the obtained Furan-PDA **2** single crystal represents the first fully structurally characterized furan-based polydiacetylene. Further research on this novel family of green conjugated polymers is currently being carried out in our laboratories. It is likely that these preliminary results will stimulate the scientific community to pursue the development of green biomass PDA-based organic electronic or sensor materials.

Supplementary Materials: The following are available online at <http://www.mdpi.com/2073-4352/9/9/448/s1>. Crystallographic information files for Compounds **1** and **2** (CIF).

Author Contributions: Conceptualization, methodology, supervision of the work, project administration, funding acquisition, investigation and writing, P.B.; synthesis of the compounds, M.C., V.O.D., and L.C.-O.; writing—review and editing, P.B. and Y.L.D.; X-ray data collection, D.F.; literature review, M.C. and V.O.D.

Funding: This research was funded by Fonds de Recherche du Québec—Nature et Technologies (FRQNT, grant No. 2019-CO-254502).

Conflicts of Interest: The authors declare no conflict of interest.

References

1. Isikgor, F.H.; Becer, C.R. Lignocellulosic Biomass: A Sustainable Platform for Production of Bio-Based Chemicals and Polymers. *Polym. Chem.* **2015**, *6*, 4497–4559. [[CrossRef](#)]
2. Decostanzi, M.; Auvergne, R.; Boutevin, B.; Caillol, S. Biobased phenol and furan derivative coupling for the synthesis of functional monomers. *Green Chem.* **2019**, *21*, 724–747. [[CrossRef](#)]
3. Gandini, A.; Lacerda, T.; Carvalho, A.; Trovatti, E. Progress of Polymers from Renewable Resources: Furans, Vegetable Oils, and Polysaccharides. *Chem. Rev.* **2016**, *116*, 1637–1669. [[CrossRef](#)]
4. Gandini, A. Polymers from Renewable Resources: A Challenge for the Future of Macromolecular Materials. *Macromolecules* **2008**, *41*, 9491–9504. [[CrossRef](#)]
5. John, G.; Nagarajan, S.; Vemula, P.K.; Silverman, J.R.; Pillai, C.K.S. Natural Monomers: A Mine for Functional and Sustainable Materials—Occurrence, Chemical Modification and Polymerization. *Prog. Polym. Sci.* **2019**, *92*, 158–209. [[CrossRef](#)]
6. Yao, K.; Tang, C. Controlled Polymerization of Next-Generation Renewable Monomers and Beyond. *Macromolecules* **2013**, *46*, 1689–1712. [[CrossRef](#)]
7. Sharif, A.; Hoque, M.E. Renewable Resource-Based Polymers. In *Bio-Based Polymers and Nanocomposites*; Sanyang, M., Jawaid, M., Eds.; Springer International: Basel, Switzerland, 2019; pp. 1–28.
8. Yuanchun, S. *Biomass: To Win the Future*; Lexington Books: Lanham, Maryland, 2013; pp. 173–174.
9. Mekonnen, T.; Mussone, P.; Khalil, H.; Bressler, D. Progress in bio-based plastics and plasticizing modifications. *J. Mater. Chem. A* **2013**, *1*, 13379–13398. [[CrossRef](#)]
10. Ten, E.; Vermerris, W. Functionalized Polymers from Lignocellulosic Biomass: State of the Art. *Polymers* **2013**, *5*, 600–642. [[CrossRef](#)]
11. Motagamwala, A.H.; Won, W.; Sener, C.; Alonso, D.M.; Maravelias, C.T.; Dumesic, J.A. Toward biomass-derived renewable plastics: Production of 2,5-furandicarboxylic acid from fructose. *Sci. Adv.* **2018**, *4*, eaap9722. [[CrossRef](#)]
12. Storz, H.; Vorlop, K.D. Bio-based plastics: Status, challenges and trends. *Appl. Agric. For. Res.* **2013**, *63*, 321–332. [[CrossRef](#)]
13. Luzi, F.; Torre, L.; Kenny, J.M.; Puglia, D. Bio- and Fossil-Based Polymeric Blends and Nanocomposites for Packaging: Structure–Property Relationship. *Materials* **2019**, *12*, 471. [[CrossRef](#)]
14. Pouloupoulou, N.; Kasmi, N.; Bikiaris, D.N.; Papageorgiou, D.G.; Floudas, G.; Papageorgiou, G.Z. Sustainable Polymers from Renewable Resources: Polymer Blends of Furan-Based Polyesters. *Macromol. Mater. Eng.* **2018**, *303*, 1800153. [[CrossRef](#)]
15. Mariscal, R.; Maireles-Torres, P.; Ojeda, M.; Sábada, I.; López Granados, M. Furfural: A renewable and versatile platform molecule for the synthesis of chemicals and fuels. *Energy Environ. Sci.* **2016**, *9*, 1144–1189. [[CrossRef](#)]
16. Lee, Y.; Kwon, E.E.; Lee, J. Polymers derived from hemicellulosic parts of lignocellulosic biomass. *Rev. Environ. Sci. Biotechnol.* **2019**, *18*, 317–334. [[CrossRef](#)]
17. Sousa, A.; Vilela, C.; Fonseca, A.; Matos, M.; Freire, C.; Gruter, G.; Coelho, J.; Silvestre, A. Biobased polyesters and other polymers from 2,5-furandicarboxylic acid: a tribute to furan excellency. *Polym. Chem.* **2015**, *6*, 5961–5983. [[CrossRef](#)]
18. Gandini, A. Furan Monomers and their Polymers: Synthesis, Properties and Applications. In *Biopolymers—New Materials for Sustainable Films and Coatings*; Plackett, D., Ed.; Wiley: New York, NY, USA, 2011; pp. 179–209.
19. De Jong, E.; Dam, M.A.; Sipos, L.; Gruter, G.-J.M. Furandicarboxylic Acid (FDCA), A Versatile Building Block for a Very Interesting Class of Polyesters. In *Biobased Monomers, Polymers, and Materials*; Smith, P.B., Gross, R.A., Eds.; ACS Symposium Series 1105; American Chemical Society: Washington, DC, USA, 2012; pp. 1–13.
20. Amarasekara, A.S. 5-Hydroxymethylfurfural Based Polymers. In *Renewable Polymers: Synthesis, Processing, and Technology*; Mittal, V., Ed.; Wiley: Hoboken, NJ, USA, 2011; pp. 381–428.

21. Gandini, A. Furans as offspring of sugars and polysaccharides and progenitors of a family of remarkable polymers: A review of recent progress. *Polym. Chem.* **2010**, *1*, 245–251. [[CrossRef](#)]
22. González-Tejera, M.J.; Sánchez de la Blanca, E.; Carrillo, I. Polyfuran conducting polymers: Synthesis, properties, and applications. *Synth. Met.* **2008**, *158*, 165–189. [[CrossRef](#)]
23. Zhang, J.; Liang, Q.; Xie, W.; Peng, L.; He, L.; He, Z.; Chowdhury, S.P.; Christensen, R.; Ni, Y. An Eco-Friendly Method to Get a Bio-Based Dicarboxylic Acid Monomer 2,5-Furandicarboxylic Acid and Its Application in the Synthesis of Poly(hexylene 2,5-furandicarboxylate) (PHF). *Polymers* **2019**, *11*, 197. [[CrossRef](#)]
24. Zeng, C.; Seino, H.; Ren, J.; Hatanaka, K.; Yoshie, N. Bio-Based Furan Polymers with Self-Healing Ability. *Macromolecules* **2013**, *46*, 1794–1802. [[CrossRef](#)]
25. Feng, Z.; Hu, J.; Yu, B.; Tian, H.; Zuo, H.; Ning, N.; Tian, M.; Zhang, L. Environmentally Friendly Method to Prepare Thermo-Reversible, Self-Healable Biobased Elastomers by One-Step Melt Processing. *ACS Appl. Polym. Mater.* **2019**, *1*, 169–177. [[CrossRef](#)]
26. Gronau, G.; Krishnaji, S.T.; Kinahan, M.E.; Giesa, T.; Wong, J.Y.; Kaplan, D.L.; Buehler, M.J. A review of combined experimental and computational procedures for assessing biopolymer structure–process–property relationships. *Biomaterials* **2012**, *33*, 8240–8255. [[CrossRef](#)]
27. Murthy, N.S. Recent developments in polymer characterization using x-ray diffraction. *Rigaku J.* **2004**, *21*, 15–24.
28. Favirov, S. Methods for the Characterization and Investigation of Polymers. In *Fundamentals of Polymer Science for Engineers*; Wiley-VCH: Weinheim, Germany, 2017; pp. 189–218.
29. Tencé-Girault, S.; Lebreton, S.; Bunau, O.; Dang, P.; Bargain, F. Simultaneous SAXS-WAXS Experiments on Semi-Crystalline Polymers: Example of PA11 and Its Brill Transition. *Crystals* **2019**, *9*, 271. [[CrossRef](#)]
30. Maini, L.; Gigli, M.; Gazzano, M.; Lotti, N.; Bikiaris, D.N.; Papageorgiou, G.Z. Structural Investigation of Poly(ethylene furanoate) Polymorphs. *Polymers* **2018**, *10*, 296. [[CrossRef](#)]
31. Mao, Y.; Kriegel, R.; Bucknall, D. The crystal structure of Poly(ethylene furanoate). *Polymer* **2016**, *102*, 308–314. [[CrossRef](#)]
32. Zhu, J.; Cai, J.; Xie, W.; Chen, P.-H.; Gazzano, M.; Scandola, M.; Gross, R.A. Poly(butylene 2,5-furan dicarboxylate), a Biobased Alternative to PBT: Synthesis, Physical Properties, and Crystal Structure. *Macromolecules* **2013**, *46*, 796–804. [[CrossRef](#)]
33. Hong, S.; Min, K.-D.; Nam, B.-U.; Park, O.O. High molecular weight bio furan-based co-polyesters for food packaging applications: Synthesis, characterization and solid-state polymerization. *Green Chem.* **2016**, *18*, 5142–5150. [[CrossRef](#)]
34. Gidron, O.; Diskin-Posner, Y.; Bendikov, M. α -Oligofurans. *J. Am. Chem. Soc.* **2010**, *132*, 2148–2150. [[CrossRef](#)]
35. Gidron, O.; Bendikov, M. α -Oligofurans: An Emerging Class of Conjugated Oligomers for Organic Electronics. *Angew. Chem. Int. Ed.* **2014**, *53*, 2546–2555. [[CrossRef](#)]
36. Gaitonde, V.; Lee, K.; Kirschmaum, K.; Sucheck, S.J. Bio-Based Bisfuran: Synthesis, Crystal Structure and Low Molecular Weight Amorphous Polyester. *Tetrahedron Lett.* **2014**, *55*, 4141–4145. [[CrossRef](#)]
37. Wang, Z.D.; Elliott, Q.; Wang, Z.; Setien, R.A.; Puttkammer, J.; Ugrinov, A.; Lee, J.; Webster, D.C.; Chu, Q.R. Furfural-Derived Diacid Prepared by Photoreaction for Sustainable Materials Synthesis. *ACS Sustain. Chem. Eng.* **2018**, *6*, 8136–8141. [[CrossRef](#)]
38. Barancelli, D.A.; Mantovani, A.C.; Jesse, C.; Nogueira, C.W.; Zeni, G. Synthesis of Natural Polyacetylenes Bearing Furan Rings. *J. Nat. Prod.* **2009**, *72*, 857–860. [[CrossRef](#)]
39. Fiandanese, V.; Bottalico, D.; Marchese, G.; Punzi, A. Synthesis of naturally occurring polyacetylenes via a bis-silylated diyne. *Tetrahedron* **2006**, *62*, 5126–5132. [[CrossRef](#)]
40. Knechtle, P.; Diefenbacher, M.; Greve, K.B. The natural diyne-furan fatty acid EV-086 is an inhibitor of fungal delta-9 fatty acid desaturation with efficacy in a model of skin dermatophytosis. *Antimicrob. Agents Chemother.* **2014**, *58*, 455–466. [[CrossRef](#)]
41. Wen, J.T.; Roper, J.M.; Tsutsui, H. Polydiacetylene Supramolecules: Synthesis, Characterization, and Emerging Applications. *Ind. Eng. Chem. Res.* **2018**, *57*, 9037–9053. [[CrossRef](#)]
42. Jelinek, R.; Ritenberg, M. Polydiacetylenes—Recent molecular advances and applications. *RSC Adv.* **2013**, *3*, 21192–21201. [[CrossRef](#)]
43. Qian, X.; Städler, B. Recent Developments in Polydiacetylene-Based Sensors. *Chem. Mater.* **2019**, *31*, 1196–1222. [[CrossRef](#)]

44. Lee, S.; Kim, J.Y.; Chen, X.; Yoon, J. Recent progress in stimuli-induced polydiacetylenes for sensing temperature, chemical and biological targets. *Chem. Commun.* **2016**, *52*, 9178–9196. [[CrossRef](#)]
45. Jelinek, R. Polydiacetylene Bio- and Chemo-Sensors. In *Encyclopedia of Analytical Chemistry*; Meyers, R.A., Ed.; Wiley: New York, NY, USA, 2019; pp. 1–24.
46. Ahn, D.J.; Lee, S.; Kim, J.-M. Rational Design of Conjugated Polymer Supramolecules with Tunable Colorimetric Responses. *Adv. Funct. Mater.* **2009**, *19*, 1483–1496. [[CrossRef](#)]
47. Yoon, B.; Lee, S.; Kim, J.-M. Recent conceptual and technological advances in polydiacetylene-based supramolecular chemosensors. *Chem. Soc. Rev.* **2009**, *38*, 1958–1968. [[CrossRef](#)]
48. Sun, X.; Chen, T.; Huang, S.; Li, L.; Peng, H. Chromatic polydiacetylene with novel sensitivity. *Chem. Soc. Rev.* **2010**, *39*, 4244–4257. [[CrossRef](#)]
49. Chen, X.; Zhou, G.; Peng, X.; Yoon, J. Biosensors and chemosensors based on the optical responses of polydiacetylenes. *Chem. Soc. Rev.* **2012**, *41*, 4610–4630. [[CrossRef](#)]
50. Huo, J.; Deng, Q.; Fan, T.; He, G.; Hu, X.; Hong, X.; Chen, H.; Luo, S.; Wang, Z.; Chen, D. Advances in polydiacetylene development for the design of side chain groups in smart material applications—A mini review. *Polym. Chem.* **2017**, *8*, 7438. [[CrossRef](#)]
51. Ortiz-Cervantes, C.; Román-Román, P.I.; Vazquez-Chavez, J.; Hernández-Rodríguez, M.; Solis-Ibarra, D. Thousand-fold Conductivity Increase in 2D Perovskites by Polydiacetylene Incorporation and Doping. *Angew. Chem. Int. Ed.* **2018**, *57*, 13882–13886. [[CrossRef](#)]
52. Marikhin, V.A.; Guk, E.G.; Myasnikova, L.P. New approach to achieving the potentially high conductivity of polydiacetylene. *Phys. Solid State* **1997**, *39*, 686–689. [[CrossRef](#)]
53. Tabata, H.; Tokoyama, H.; Yamakado, H.; Okuno, T. Preparation and properties of two-legged ladder polymers based on polydiacetylenes. *J. Mater. Chem.* **2012**, *22*, 115–122. [[CrossRef](#)]
54. Xu, X.-Q.; He, Y.; Liu, H.; Wang, Y. Polydiacetylene–Polyurethane Crisscross Elastomer as an Intrinsic Shape Memory Conductive Polymer. *ACS Macro Lett.* **2019**, *8*, 409–413. [[CrossRef](#)]
55. Zhang, X.; Dong, H.; Hu, W. Organic Semiconductor Single Crystals for Electronics and Photonics. *Adv. Mater.* **2018**, *30*, 1801048. [[CrossRef](#)]
56. Ulaganathan, M.; Varghese Hansen, R.; Drayton, N.; Hingorani, H.; Kutty, R.G.; Joshi, H.; Sreejith, S.; Liu, Z.; Yang, J.; Zhao, Y. Photopolymerization of Diacetylene on Aligned Multiwall Carbon Nanotube Microfibers for High-Performance Energy Devices. *ACS Appl. Mater. Interfaces* **2016**, *8*, 32643–32648. [[CrossRef](#)]
57. Takami, K.; Kuwahara, Y.; Ishii, T.; Akai-Kasaya, M.; Saito, A.; Aono, M. Significant increase in conductivity of polydiacetylene thin film induced by iodine doping. *Surface Sci. Lett.* **2005**, *591*, 273–279. [[CrossRef](#)]
58. Yao, Y.; Dong, H.; Liu, F.; Russel, T.P.; Hu, W. Approaching Intra- and Interchain Charge Transport of Conjugated Polymers Facilely by Topochemical Polymerized Single Crystals. *Adv. Mater.* **2017**, *29*, 1701251. [[CrossRef](#)] [[PubMed](#)]
59. Matsuda, H.; Nakanishi, H.; Kato, S.-I.; Kato, M. Conductivity of polydiacetylene with π -conjugation between polymer backbone and substituents. *J. Polym. Sci. Part A Polym. Chem.* **1987**, *25*, 1663–1669. [[CrossRef](#)]
60. Tang, Z.; Li, M.; Song, M.; Jiang, L.; Li, J.; He, Y.; Zhou, L. Good conductivity of a single component polydiacetylene film. *Org. Electron.* **2017**, *49*, 174–178. [[CrossRef](#)]
61. Tahir, M.N.; Nyayachavadi, A.; Morin, J.-F.; Rondeau-Gagné, S. Recent progress in the stabilization of supramolecular assemblies with functional polydiacetylenes. *Polym. Chem.* **2018**, *9*, 3019–3028. [[CrossRef](#)]
62. Halasz, I. Single-Crystal-to-Single-Crystal Reactivity: Gray, Rather than Black or White. *Cryst. Growth Des.* **2010**, *10*, 2817–2823. [[CrossRef](#)]
63. Lauher, J.W.; Fowler, F.W. Single-Crystal-to-Single-Crystal Topochemical Polymerizations by Design. *Acc. Chem. Res.* **2008**, *41*, 1215–1229. [[CrossRef](#)] [[PubMed](#)]
64. Curtis, S.M.; Le, N.; Nguyen, T.; Ouyang, X.; Tran, T.; Fowler, F.W.; Lauher, J.W. What have We Learned about Topochemical Diacetylene Polymerizations? *Supramol. Chem.* **2005**, *17*, 31–36. [[CrossRef](#)]
65. Biradha, K.; Santra, R. Crystal engineering of topochemical solid state reactions. *Chem. Soc. Rev.* **2013**, *42*, 950. [[CrossRef](#)]
66. Chaudhary, A.; Mohammad, A.; Mobin, S.M. Recent Advances in Single-Crystal-to-Single-Crystal Transformation at the Discrete Molecular Level. *Cryst. Growth Des.* **2017**, *17*, 2893–2910. [[CrossRef](#)]
67. Hay, A.S. Oxidative Coupling of Acetylenes II. *J. Org. Chem.* **1962**, *27*, 3320–3321. [[CrossRef](#)]
68. Baughman, R.H. Solid-State Synthesis of Large Polymer Single-Crystals. *J. Polym. Sci. Polym. Phys. Ed.* **1974**, *12*, 1511–1535. [[CrossRef](#)]

69. Turowska-Tyrk, I.; Grześniak, K.; Trzop, E.; Zych, T. Monitoring structural transformations in crystals. Part 4. Monitoring structural changes in crystals of pyridine analogs of chalcone during [2+2]-photodimerization and possibilities of the reaction in hydroxy derivatives. *J. Solid State Chem.* **2003**, *174*, 459–465. [[CrossRef](#)]
70. Bertault, M.; Canceill, J.; Collet, A.; Toupet, L. Synthesis and Solid-state Polymerization Properties of Symmetrical and Unsymmetrical Diacetylene Derivatives containing a 'Polymerogenic' Side Group. *J. Chem. Soc. Chem. Commun.* **1988**, 163–166. [[CrossRef](#)]
71. Rigas, G.-P.; Payne, M.P.; Anthony, J.E.; Horton, P.N.; Castro, A.F. Spray printing of organic semiconducting single crystals. *Nat. Commun.* **2016**, *7*, 13531. [[CrossRef](#)] [[PubMed](#)]
72. Cao, X.; Zhao, K.; Chen, L.; Liu, J.; Han, Y. Conjugated polymer single crystals and nanowires. *Polym. Cryst.* **2019**, e10064. [[CrossRef](#)]



© 2019 by the authors. Licensee MDPI, Basel, Switzerland. This article is an open access article distributed under the terms and conditions of the Creative Commons Attribution (CC BY) license (<http://creativecommons.org/licenses/by/4.0/>).